NAVAL POSTGRADUATE SCHOOL
Monterey, California

THESIS

Direct Detection and Coherent Optical Systems Employing Error-Correction Coding

by

Eui-Sik Hwang

June 1994

Thesis Advisor: Tri T. Ha
Co-Advisor: Randy L. Borchardt

REPORT DOCUMENTATION PAGE

Public reporting burden for this collection of information is estimated to average 1 hour per response, including the time for reviewing instructions, searching existing data sources, gathering and maintaining the data needed, and completing and reviewing the collection of information. Send comments regarding this burden estimate or any other aspect of this collection of information, including suggestions for reducing this burden, to Washington Headquarters Services, Directorate for Information Operations and Reports, 1215 Jefferson Davis Highway, Suite 1204, Arlington, VA 22202-4302, and to the Office of Management and Budget, Paperwork Reduction Project (0704-0188), Washington, DC 20503.

1. AGENCY USE ONLY (Leave blank)	2. REPORT DATE June 1994	3. REPORT TYPE AND DATES COVERED Master's Thesis

4. TITLE AND SUBTITLE
DIRECT DETECTION AND COHERENT OPTICAL SYSTEMS
EMPLOYING ERROR-CORRECTION CODING

5. FUNDING NUMBERS

6. AUTHOR(S)
Hwang, Eui-Sik

7. PERFORMING ORGANIZATION NAME(S) AND ADDRESS(ES)

Naval Postgraduate School
Monterey, CA 93943-5000

8. PERFORMING ORGANIZATION REPORT NUMBER

9. SPONSORING/MONITORING AGENCY NAME(S) AND ADDRESS(ES)

10. SPONSORING/MONITORING AGENCY REPORT NUMBER

11. SUPPLEMENTARY NOTES
The views expressed in this thesis are those of the author and do not reflect the
official policy or position of the Department of Defense or the United States Government.

12a. DISTRIBUTION/AVAILABILITY STATEMENT
Approved for public release; distribution unlimited.

12b. DISTRIBUTION CODE

13. ABSTRACT (Maximum 200 words)
We evaluate the bit error probability of coded lightwave systems employing direct detection with OOK modulation, and coherent systems with FSK modulation and noncoherent detection. Block codes, convolutional codes, and concatenated codes are investigated. For direct systems, both hard and soft decoding are considered. Only hard decoding is employed in coherent optical systems.

14. SUBJECT TERMS bit error probability, coding			15. NUMBER OF PAGES 40
			16. PRICE CODE

17. SECURITY CLASSIFICATION OF REPORT UNCLASSIFIED	18. SECURITY CLASSIFICATION OF THIS PAGE UNCLASSIFIED	19. SECURITY CLASSIFICATION OF ABSTRACT UNCLASSIFIED	20. LIMITATION OF ABSTRACT UL

Direct Detection and Coherent Optical Systems Employing Error-Correcting Coding

by

Eui-Sik Hwang
Lieutenant, Korean Navy
B. S., R.O.K. Naval Academy, 1989

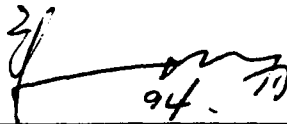Submitted in partial fulfillment of the
requirements for the degree of

MASTER OF SCIENCE IN ENGINEERING ACOUSTICS
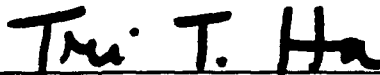
from the

NAVAL POSTGRADUATE SCHOOL

June 1994

Author: _____
Eui-Sik Hwang

Approved by: _____
Tri T. Ha, Thesis Advisor

_____
Randy L. Borchardt, Co-Advisor

_____
James Vincent Sanders, Acting Chairman
Engineering Acoustic Academic Committee

ABSTRACT

We evaluate the bit error probability of coded lightwave systems employing direct detection with OOK modulation, and coherent optical systems with FSK modulation and noncoherent detection. Block codes, convolutional codes, and concatenated codes are investigated. For direct detection systems, both hard and soft decoding are considered. Only hard decoding is employed in coherent optical systems.

iii

TABLE OF CONTENTS

LIST OF FIGURES

I. INTRODUCTION

The benefits of forward error-correction coding for radio communications in an additive white Gaussian noise (AWGN) channel are well documented [1-3]. With the state-of-the-art technology of Application Specific Integrated Circuits (ASIC), both block coding and convolutional coding can be implemented at very high bit rates. Block coding can be implemented at Gb/s data rates and convolutional coding at hundreds of Mb/s data rates. This opens the possibility for employing FEC in lightwave systems to compensate for the loss in the link budget or to relax the laser linewidth requirement in coherent optical systems [4-5].

In this study, we explore the benefit of FEC for direct detection lightwave systems employing on-off-keying (OOK) modulation, and coherent optical systems employing frequency-shift keying (FSK) with envelope detection corrupted by phase noise. Our work was derived explicitly from [19].

Of practical importance is the use of concatenated codes. Concatenated codes allow the use of two relatively short codes with modest error-correcting capability, one as the inner code and the other as the outer code to achieve a large coding gain. Short codes with modest error-correcting capability simplify decoder design at very high data rates and thus reduce the implementation cost. Concatenated codes also allow the use of a short constraint length convolutional code as the inner code with soft decoding and a short Reed-Solomon (RS) code with modest error-correcting capability as the outer code. This scheme can achieve a large coding gain which otherwise can only be achieved with a long constraint length convolutional code or a long RS code with large error-correcting capability.

1

2

II. BIT ERROR PROBABILITY OF DIRECT DETECTION LIGHTWAVE SYSTEMS

A. OOK MODULATION

The direct detection OOK receiver model to be analyzed is given in Fig. 1. The photodiode detector has a responsivity $\mathcal{R} = \eta q / h_f$ (A/W) where η is the quantum efficiency which is near unity for $p - i - n$ diodes, $q = 1.6 \times 10^{-19}$ C is the electron charge, $h = 6.626 \times 10^{-34}$ J S is Planck's constant, and f is the laser frequency. The current produced by the photodiode is amplified by a low noise amplifier and integrated by the integrator. With soft decoding, the analog samples from the integrator are processed by the soft decoder. With hard decoding, the integrator's samples are first detected by a threshold detector to provide hard quantized samples to the hard decoder.

In practice, the shot noise and dark currents produced by the photodiode are negligible compared to the thermal noise current generated by the low noise amplifier. Therefore, they are ignored in our analysis. The complex envelope of the OOK lightwave signal incident upon the photodiode detection during a coded bit interval T is

$$s_i(t) = \sqrt{P}\, b_i e^{j\theta(t)} \qquad i = 0, 1 ; \quad 0 < t < T \tag{1}$$
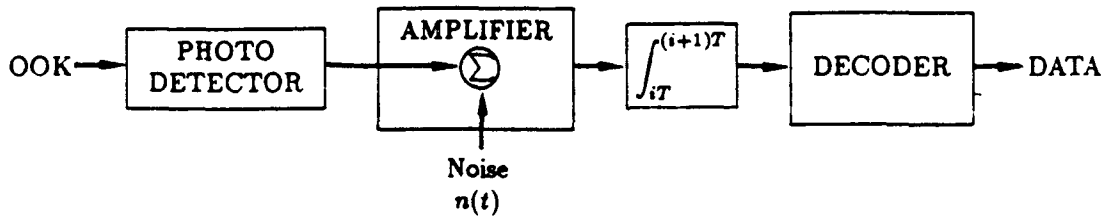
Figure 1: Coded OOK direct detection receiver structure.

where P is peak power, $b_0 = \sqrt{\rho/(1+\rho)}$, $b_1 = \sqrt{1/(1+\rho)}$ and ρ is the laser extinction ratio. The output of the integrator is

$$Y_i = \mathcal{R} \int_0^T |s_i(t)|^2 dt + \int_0^T n(t) dt \tag{2}$$

where $n(t)$ is the thermal noise current with spectral density N_0 (A^2/Hz). Substituting (1) into (2) and denote

$$N = \int_0^T n(t) dt \tag{3}$$

we obtain

$$Y_i = \mathcal{R} P T b_i^2 + N \tag{4}$$

Note that N is a Gaussian random variable with zero mean and variance $\sigma^2 = N_0 T$. We assume that the soft decoding is done by a maximum likelihood soft decoder using the analog (unquantized) samples Y_i in (4). For hard decoding, a bit decision at the output of the threshold detector employing a threshold setting α is produced with channel transition probability as follows:

$$
\begin{aligned}
p &= \frac{1}{2} Pr\{Y_0 > \alpha\} + \frac{1}{2} Pr\{Y_1 \le \alpha\} \\
&= \frac{1}{2} Q\left(\frac{\alpha - \mathcal{R} P T b_0^2}{\sqrt{N_0 T}}\right) + \frac{1}{2} Q\left(\frac{\mathcal{R} P T b_1^2 - \alpha}{\sqrt{N_0 T}}\right)
\end{aligned}
\tag{5}
$$

where $Q(x)$ is give by

$$Q(x) = \frac{1}{\sqrt{2\pi}} \int_x^\infty e^{-z^2/2} dz \tag{6}$$

The minimum value of p at the optimum threshold setting $\alpha_{opt} = \mathcal{R} P T (b_1^2 + b_0^2)/2$ is

$$
\begin{aligned}
p + Q\left(\frac{\mathcal{R} P T (b_1^2 - b_0^2)}{2\sqrt{N_0 T}}\right) \\
= Q\left(\frac{1}{2} SNR \sqrt{r}\right)
\end{aligned}
\tag{7}
$$

4

where

$$SNR = \mathcal{R}P(b_1^2 - b_0^2)\sqrt{\frac{T_b}{N_0}} \tag{8}$$

is the signal-to-noise ratio at the threshold detector input, r is the code rate, and T_b is the bit interval.

B. CODING

Assuming that the decoding is accomplished by a maximum likelihood decoder, then the bit error probability of the decoded OOK signals employing block code (n, k) is upper bounded by

$$P_b < \sum_{j=1}^{n} \frac{j}{n} n_j P_j \tag{9}$$

where n_j is the number of code words of weight j, and P_j is the probability that the distance between the received sequence and a weight-j code word is less than the distance to an all-zero code word

For a convolutional code with rate k/n, the bit error probability is upper bounded by [1-3]

$$P_b < \frac{1}{k} \sum_{j=d_f}^{\infty} \omega_j P_j \tag{10}$$

where ω_j is the total information weight of all code paths of weight j, d_f is the free distance of the code, and P_j is the probability that the all-zero path is eliminated by a path of weight j merging with it.

With hard decoding, the probability P_j in (9) and (10) is given by

$$P_j = \begin{cases} \sum_{i=(j+1)/2}^{j} \binom{j}{i} p^i (1-p)^{j-i}, & j \text{ odd} \\ \\ \frac{1}{2} \binom{j}{j/2} p^{j/2}(1-p)^{j/2} + \sum_{i=j/2+1}^{j} \binom{j}{i} p^i (1-p)^{j-i}, & j \text{ even} \end{cases} \tag{11}$$

5

where p is the channel transition probability in (7). Alternatively P_2 in (9) can be calculated by the following upper bound

$$P_b < \sum_{j=t+1}^{n} \frac{j+t}{n} \binom{n}{j} p^j (1-p)^{n-j} \qquad (12)$$

where t is the error correcting capability of the block code.

For soft decoding, the decoder selects the code word (or code path) at minimum Euclidean distance from the received sequence. Thus, P_j in (9)–(10) is the probability that the Euclidean distance between the received sequence Y and weight-j code word X_j is less than the Euclidean distance to the assumed transmitted all-zero code word X_0. Thus

$$P_j = Pr\left\{\|Y - X_j\|^2 < \|Y - X_0\|^2\right\} \qquad (13)$$

where X_j is a vector with j components, each of value $\mathcal{R}PTb_1^2$, represented bit ones, and the remaining components, each of value $\mathcal{R}PTb_0^2$, represented bit zeros; the vector X_0 represents the assumed transmitted all-zero sequence with each component assuming the value $\mathcal{R}PTb_0^2$. The received vector is $Y = X_0 + N$ where N is the zero mean Gaussian noise vector, each component has variance $\sigma^2 = N_0 T$.

We note that by using $Y = X_0 + N$ in (12) we have

$$
\begin{aligned}
P_j &= Pr\left\{\|N - (X_j - X_0)\|^2 < \|N\|^2\right\} \\
&= Pr\left\{\|N\|^2 + \|X_j - X_0\|^2 - 2Re\left\{\langle N, X_j - X_0\rangle\right\} < \|N\|^2\right\} \\
&= Pr\left\{2Re\left\{\langle N, X_j - X_0\rangle\right\} \geq \|X_j - X_0\|^2\right\} \\
&= Pr\left\{Re\left\{\left\langle N, \frac{X_j - X_0}{\|X_j - X_0\|}\right\rangle\right\} > \frac{1}{2}\|X_j - X_0\|\right\} \qquad (14)
\end{aligned}
$$

where $\langle N, X_j - X_0\rangle$ is the inner product of the two vectors N and $X_j - X_0$. We remark that $Re\left\{\langle N, (X_j - X_0)/\|X_j - X_0\|\rangle\right\}$ is the sum of zero mean Gaussian

random variables, each with variance $\sigma^2 = N_0 T$, and $(X_j - X_0)/\|X_j - X_0\|$ is a unit length vector. Thus, it is a zero mean Gaussian variable with variance $\sigma^2 = N_0 T$. Hence

$$
\begin{aligned}
P_j &= Q\left(\frac{\|X_j - X_0\|}{2\sqrt{N_0 T}}\right) \\
&= Q\left(\frac{\mathcal{R}PT(b_1^2 - b_0^2)\sqrt{j}}{2\sqrt{N_0 T}}\right) \\
&= Q\left(\frac{1}{2}\mathcal{R}P(b_1^2 - b_0^2)\sqrt{j\frac{T}{N_0}}\right) \\
&= Q\left(\frac{1}{2}SNR\sqrt{jr}\right) \quad (15)
\end{aligned}
$$

where r is the code rate and SNR is given in (8).

The above results are applied to various codes to study their effectiveness. Figure 2 shows the bit error probability P_b versus signal-to-noise ratio SNR for the (7, 4) Hamming code and the concatenated (7, 4)/(15, 11) Hamming/Reed-Solomon codes with the Hamming code as the inner code. With hard decoding the Hamming code provides very small coding gain. On the other hand, the coding gain at $P_b = 10^{-15}$ is about 2.3 dB for the concatenated codes with soft decoding for the Hamming code. The coding gain at $P_b = 10^{-15}$ is almost 3 dB as shown in Fig. 3 for the concatenated (31, 27)/(27, 23) RS/RS with hard decoding where the (27, 23) is the shortened outer code.

Figure 4 shows the performance of a convolutional code with rate 3/4 and constraint length $\nu = 2$ and $\nu = 5$. The shorter constraint length $\nu = 2$ is more suitable for high data rates. The coding gain at $P_b = 10^{-15}$ is about 1.5 dB for $\nu = 2$ and 2.5 dB for $\nu = 5$. Large coding gain can be obtained with the concatenated rate 3/4 convolutional/(31, 27) RS codes with the convolutional code as the inner code

7

as in Fig. 5. A coding gain of about 2.8 dB and 4 dB can be achieved at $P_b = 10^{-15}$ with soft decoding for the convolutional code with $\nu = 2$ and $\nu = 5$, respectively.
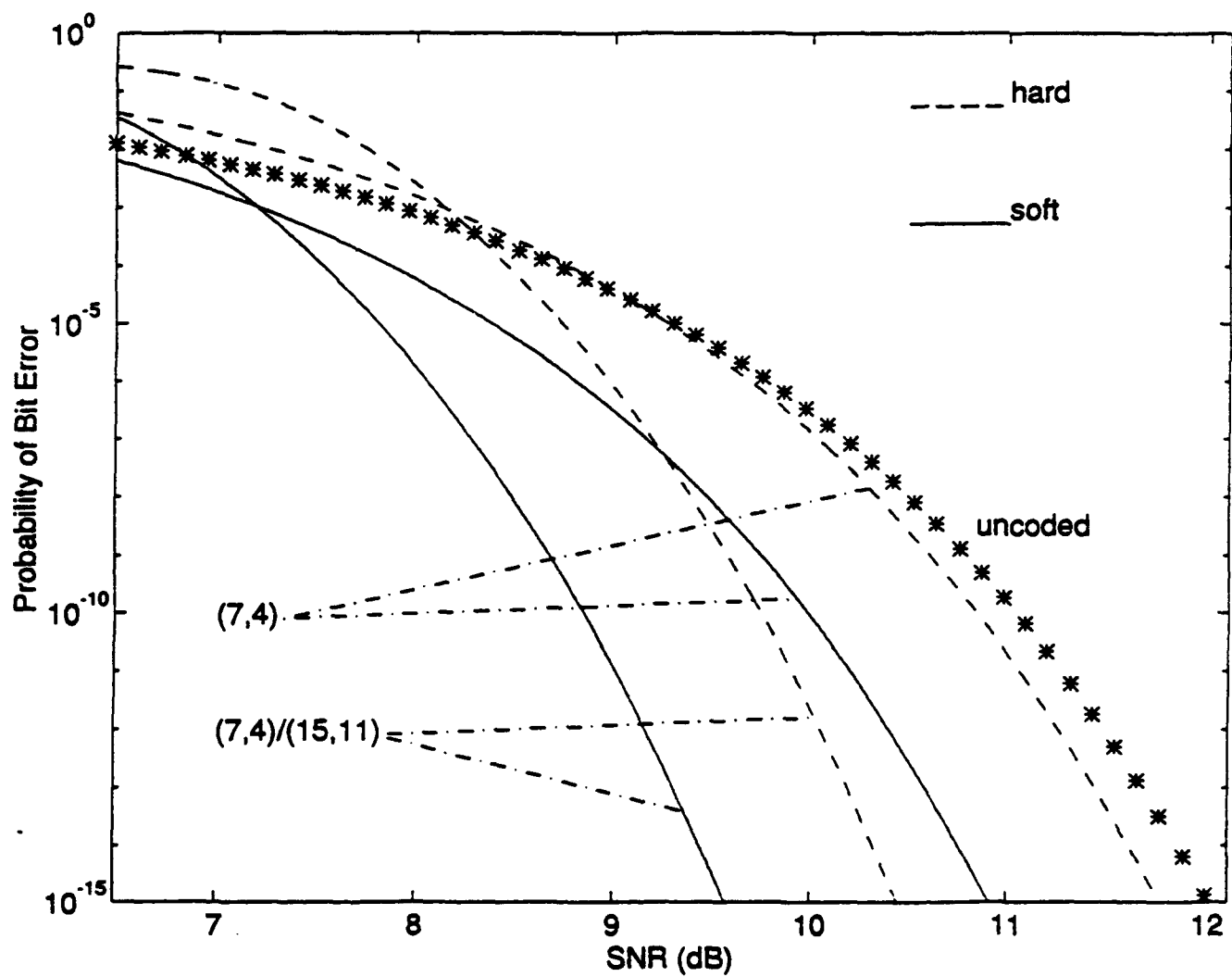
Figure 2: Coded P_b versus SNR for direct detection systems employing (7, 4) Hamming code, (15, 11) Reed-Solomon code, and concatenated (7, 4)/(15, 11) Hamming/Reed-Solomon codes.

9

Figure 3: Coded P_b versus SNR for direct detection systems employing (31, 27)/(27, 23) Reed-Solomon/Reed-Solomon codes.

Figure 4: Coded P_b versus SNR for direct detection systems employing rate 3/4 convolutional code with constraint lengths $\nu = 2, 5$.
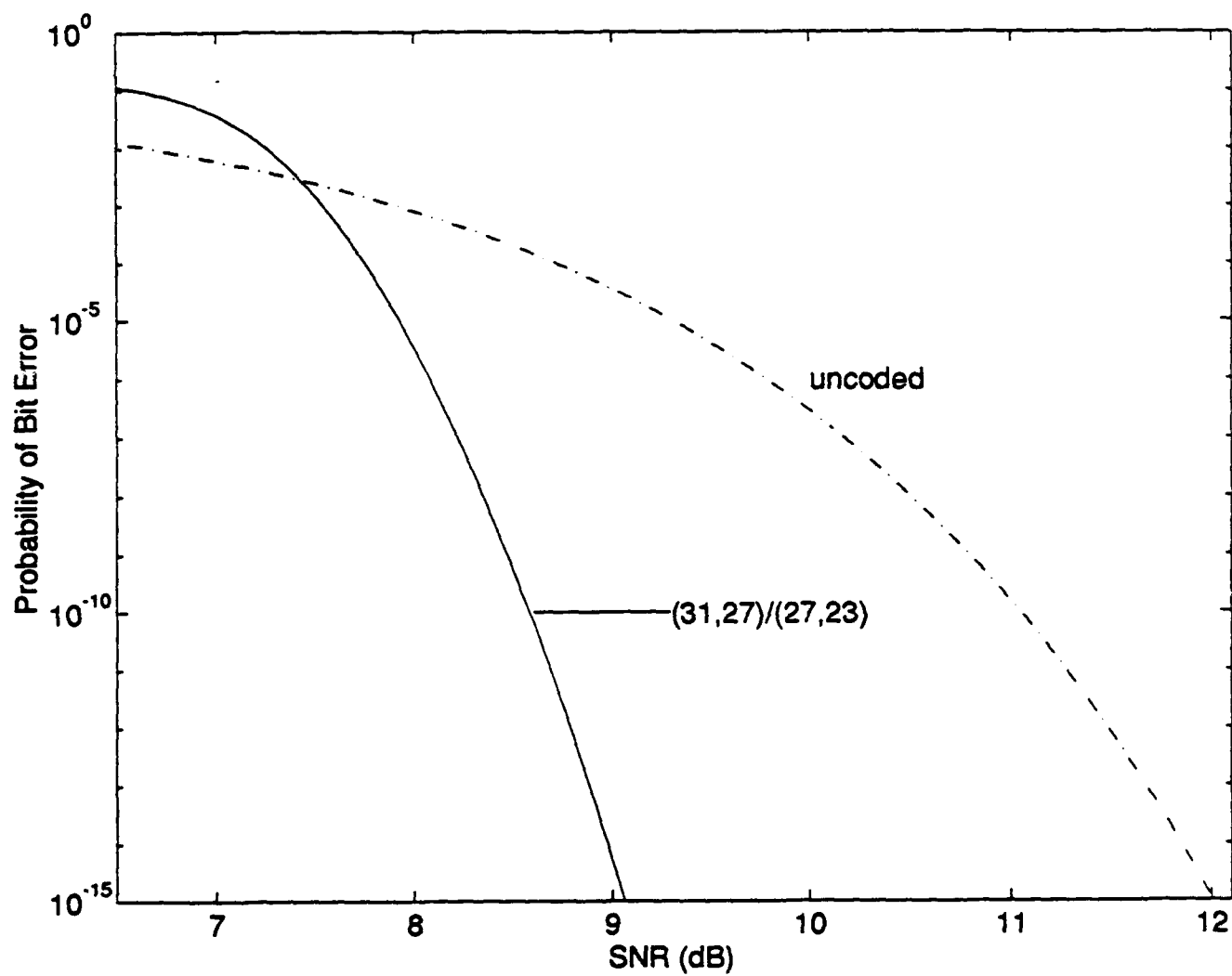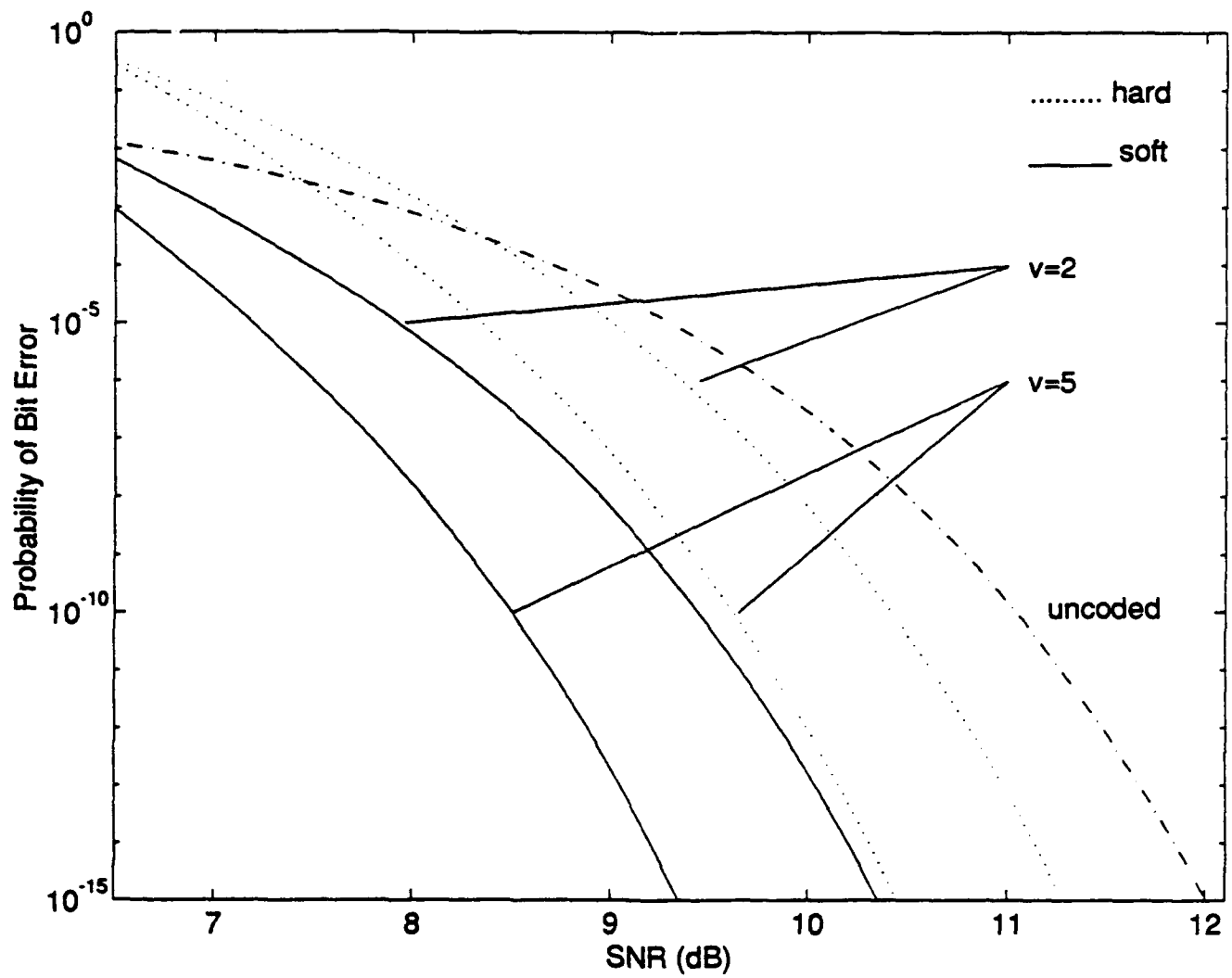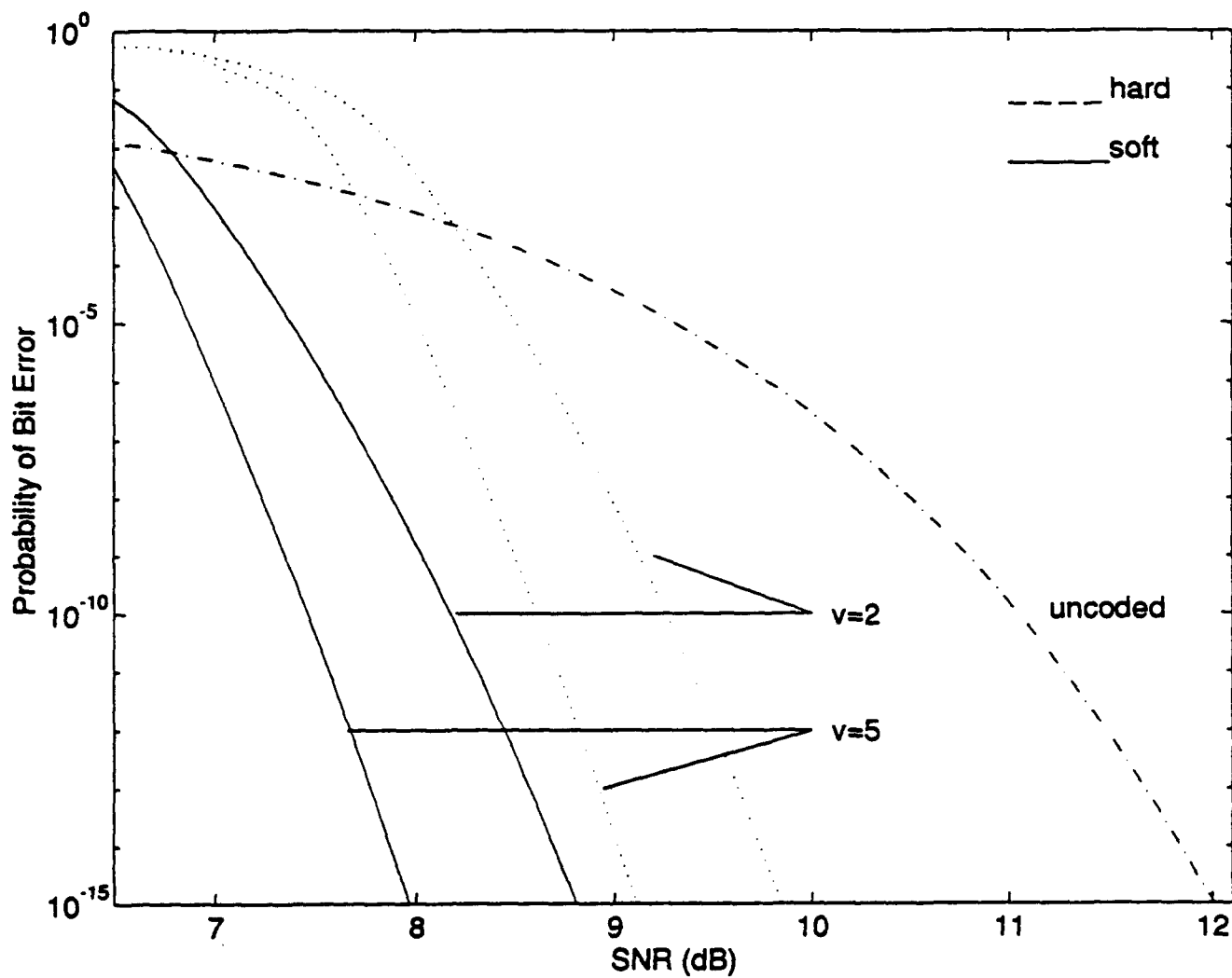
11

Figure 5: Coded P_b versus SNR for direct detection systems employing concatenated rate 3/4 convolutional code/(31, 27) Reed-Solomon codes.

III. BIT ERROR PROBABILITY OF COHERENT OPTICAL FSK SYSTEMS WITH NONCOHERENT DETECTION

Heterodyne and homodyne (coherent) lightwave systems are largely affected by the combined laser phase noise of the source and local laser oscillators. The performance deteriorates as the linewidth bit time βT_b increases where β (Hz) is the combined laser linewidth of the source and local lasers and T_b (s) is the bit time [6-10]. Coherently detected signals suffer much more from the phase noise than noncoherently detected signals. The phase noise which can be modeled as a Brownian motion process causes signal fading and broadens the signal spectrum. Both effects can be compensated to a large extent by using a wider predetection filter to pass more of the signal power and an averaging postdetection filter to provide time diversity and thus alleviating the signal fading effect. Such a technique was investigated in [11-12] for heterodyne lightwave systems employing ASK and wideband FSK with noncoherent detection, and in [13] for homodyne lightwave systems. The use of time diversity is equivalent to the use of simple repetition codes. Since simple repetition codes can provide a good improvement as reported in [11-12], one would naturally expect an even larger improvement when more powerful and efficient codes are used.

In this part we investigate the performance of heterodyne lightwave systems using wideband orthogonal FSK with noncoherent detection and error-correction codes. We will show that coding can provide a substantial improvement in the face of the phase noise and shot noise modeled as a zero-mean Gaussian process with power spectral density (PSD) $N_0/2$ (W/Hz). Furthermore, coding can relax the βT_b

13

requirement a great deal thus enabling the use of inexpensive lasers with a much larger linewidth than that required by an uncoded system. For total generality we consider both time diversity and coding for the system under investigation as shown in Fig. 6. We assume that the frequency spacing $|f_0 - f_1|$ is much larger than $1/T'$ where T' is the integration time and is also the sampling time at the summer outputs. The time T' is selected such that the code symbol time $T = rT_b = MT'$ where M is a positive integer and r is the code rate. Time diversity of the postdetection filter is modeled by summing M independent samples of a coded bit after envelope detection. The output samples are fed to the decoder which can make a hard decision or soft decision on the received codewords. Equivalently, each branch of the demodulator in Fig. 6 can be replaced by a bandpass integrator followed by a square-law envelope detector [12]. In the following section we derive the channel transition probability. We provide a simple derivation as an alternative to the one in [12].

For mathematical convenience we adopt the envelope notation of a real signal. Thus, the summer outputs of the signal-present upper branch and the signal-absent lower branch in Fig. 6 with integration time T' are

$$Y_0 = \sum_{k=1}^{M} |X_k + n_{c0k} + jn_{s0k}|^2 \tag{16}$$

$$Y_1 = \sum_{k=1}^{M} |n_{c1k} + jn_{s1k}|^2 \tag{17}$$

where Z_k is given by

$$Z_k = \frac{A}{2} \int_{(k-1)T}^{kT} e^{j\theta(t)} dt \tag{18}$$

and all the in-phase and quadrature noise samples n_{cik}, $n_{sik}(i = 0, 1; k = 1, 2, \cdots, M)$ are independent and identically distributed (i.i.d.) zero-mean Gaussian random variables (R.V.) with variance $N_0 T/4$. The laser phase noise process $\theta(t)$ can be characterized as a zero-mean Gaussian process with variance $2\pi\beta t$ [16], where β is the combined linewidth of the source and local laser oscillators.

14
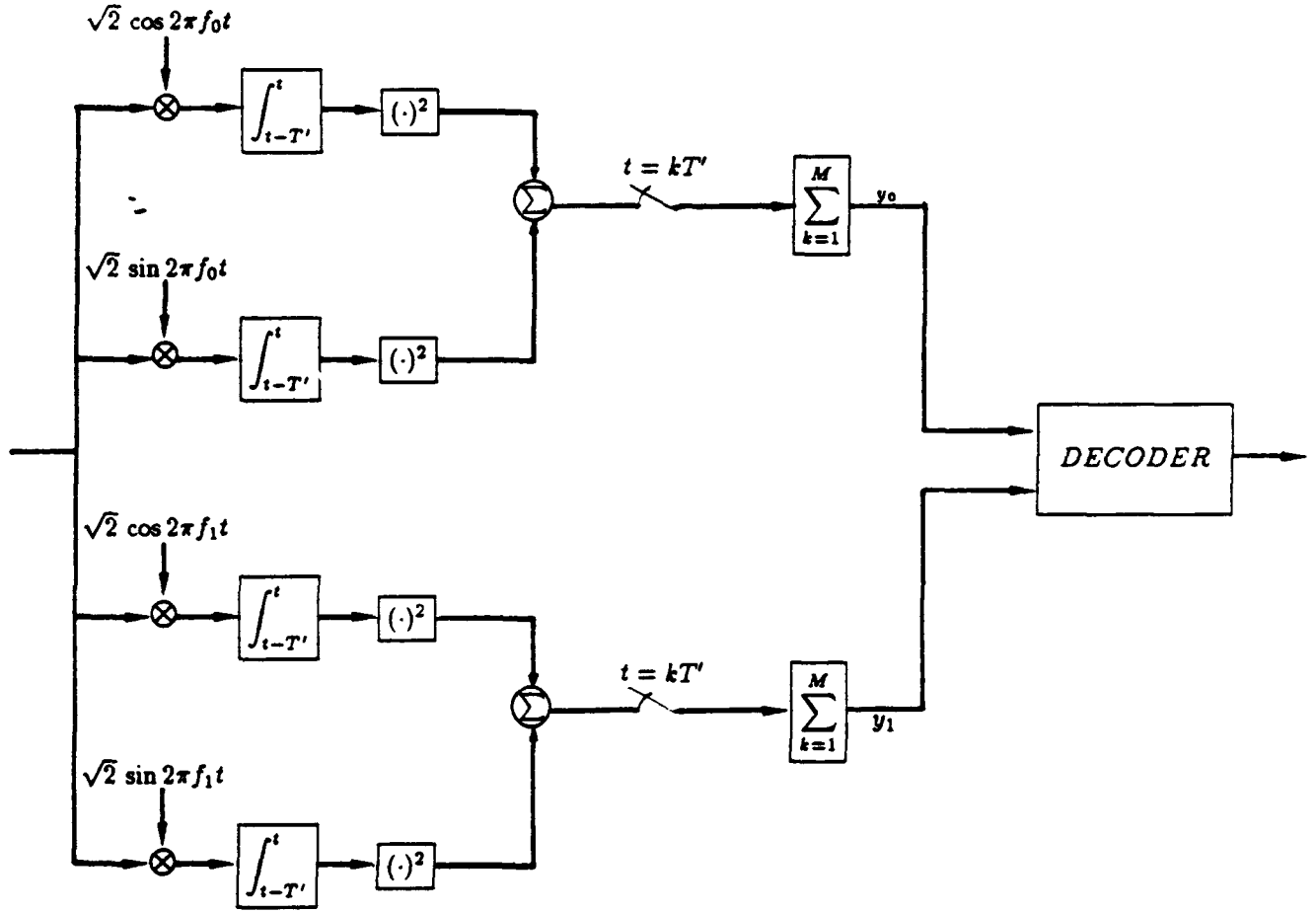
Figure 6: Coded coherent optical FSK receiver structure.

Since Y_1 is the sum of squares of $2M$ i.i.d. Gaussian R.V.s with zero mean and variance $\sigma^2 = N_0 T'/4$, Y_1 is chi-square distributed with the following probability density function (pdf) [14]

$$f_{y_1} = \frac{1}{(M-1)!2^M \sigma^{2M}} y_1^{M-1} e^{-y_1/2\sigma^2}, \qquad y_1 \geq 0 \qquad (19)$$

On the other hand, Y_0 is the sum of squares of M independent Gaussian R.V.s with variance σ^2 and mean $Re\{X_k\}$ and M independent Gaussian R.V.s with the same variance σ^2 but with mean $I_m\{X_k\}$. Here $Re\{X_k\}$ and $I_m\{X_k\}$ denote the real and

imaginary parts of X_k, respectively. Thus, Y_0 is non-central chi-square distributed with the following conditional pdf [14]

$$f_{Y_0}(y_0|v) = \frac{1}{2\sigma^2}\left(\frac{y_0}{v}\right)^{(M-1)/2} e^{-(y_0+v)/2\sigma^2} I_{M-1}\left(\frac{\sqrt{vy_0}}{\sigma^2}\right), \qquad y_0 \geq 0 \qquad (20)$$

where $I_{M-1}(\cdot)$ is the $(M-1)$th-order modified Bessel function of the first kind, and v is the value assumed by the random variable V defined as

$$V = \sum_{k=1}^{M} |Z_k|^2 \qquad (21)$$

The conditional channel transition probability of error is given by

$$p(v) = Pr\{Y_1 \geq Y_0|v\}$$

$$= \int_0^\infty \int_{y_0}^\infty f_{Y_1}(y_1)f_{Y_0}(y_0|v)dy_1 dy_0 \qquad (22)$$

The inner integral can be evaluated as follows:

$$\int_{y_0}^\infty f_{Y_1}(y_1)dy_1 = e^{-y_0/2\sigma^2}\sum_{k=0}^{M-1}\left(\frac{y_0}{2\sigma^2}\right)^k \frac{1}{k!} \qquad (23)$$

Substituting (20) and (23) into (21), we obtain

$$p(w) = \frac{e^{-w}}{w^{(M-1)/2}}\sum_{k=0}^{M-1}\frac{1}{k!}\int_0^\infty x^{(M-1)/2+k}e^{-2x}I_{M-1}(2\sqrt{wx})dx \qquad (24)$$

where w is the value assumed by the random variable W as defined as

$$W = \frac{V}{2\sigma^2} = \frac{1}{2\sigma^2}\sum_{k=1}^{M} |Z_k|^2 \qquad (24)$$

Using the identity [15]

$$\int_0^\infty x^{\nu/2+n}e^{\xi x}I_\nu(2\alpha\sqrt{x})dx = n!\alpha^\nu e^{\alpha^2/\xi}\xi^{-n-\nu-1}L_n^\nu\left(-\frac{\alpha^2}{\gamma}\right) \qquad (26)$$

where

$$L_n^\nu(s) = \sum_{m=0}^{n}(-1)^m \binom{n+\nu}{n-m}\frac{s^m}{m!} \qquad (27)$$

16

in (24) we obtain

$$p(w) = \frac{e^{-w/2}}{2M} \sum_{k=0}^{M-1} \frac{1}{2^k} \sum_{m=0}^{k} \binom{k+M-1}{k-m} \frac{(w/2)^m}{m!}$$

$$= \frac{e^{-w/2}}{2M} \sum_{n=0}^{M-1} \frac{(w/2)^n}{n!} \sum_{k=n}^{M-1} \binom{k+M-1}{k-n} \frac{1}{2^k} \qquad (28)$$

Define

$$SNR = A^2 T_b/2N_0 , \qquad y = \sum_{k=1}^{M} X_k(rc/M)$$

where r is the code rate, $c = 2\pi\beta T_b$ and X_k is given by

$$X_k(rc/M) = \left| \int_{k-1}^{k} e^{j\sqrt{rc/M}\psi(t)}dt \right|^2 \qquad (29)$$

with $\psi(t)$ as a zero mean Gaussian process of variance t; we can express the conditional channel transition probability in (28) as follows:

$$p(y) = \frac{e^{-(SNR)ry/2M}}{2M} \sum_{n=0}^{M-1} \frac{[(SNR)ry/2M]^n}{n!} \sum_{k=n}^{M-1} \binom{k+M-1}{k-n} \frac{1}{2^k} \qquad (30)$$

The channel transition probability is given by

$$p = E\{p(y)\} = \int_0^\infty p(y)f_Y(y)dy \qquad (31)$$

where $f_Y(y)$ is the probability density function of y and can be calculated by the method given in [12]. Figure 7 shows $f_Y(y)$ for $M = 2$, $c = 1$, and $c = 4$ for the uncoded case.

The transition probability p in (31) is applied to (9)–(12) to evaluate the effectiveness of various codes for coherent optical systems. Figure 8 shows the bit error probability P_b versus the signal-to-noise ratio SNR for $M = 1$ and-$c = 1$ (small phase noise) with hard decoding (15, 11) and (31, 27) RS codes and (31, 27)/(27, 23) concatenated RS/RS codes. It is seen that coding provides an excellent performance as compared to an uncoded system, especially for the concatenated code. When

17

$M = 2$, that is, the bandwidth of the integrators is twice the coded rate, more signal power passes through the demodulator and the performance of an uncoded system as shown in Fig. 9 improves remarkably over an uncoded system for $M = 1$ in Fig. 8. In this situation the improvement in performance when RS codes are employed is less than that in Fig. 8 but the improvement is still considerable, especially for the concatenated $(31, 27)/(27, 23)$ RS/RS codes. When the phase noise is large as shown in Fig. 10 for $c = 4$, the use of both RS codes and larger integrator bandwidth $M = 2$ achieves considerable improvement for the $(15, 11)$ and $(31, 27)$ RS codes and the concatenated $(31, 27)/(27, 23)$ RS/RS codes. Figures 11 and 12 show the performance of rate $3/4$ convolutional codes with hard decoding for $M = 2$, and $c = 1$ and $c = 4$, respectively. It is observed that when the constraint length is small, $\nu = 2$, the improvement is small. The performance of rate $3/4$, $\nu = 5$ convolutional codes is slightly less than that of RS codes $(15, 11)$ or $(31, 27)$.
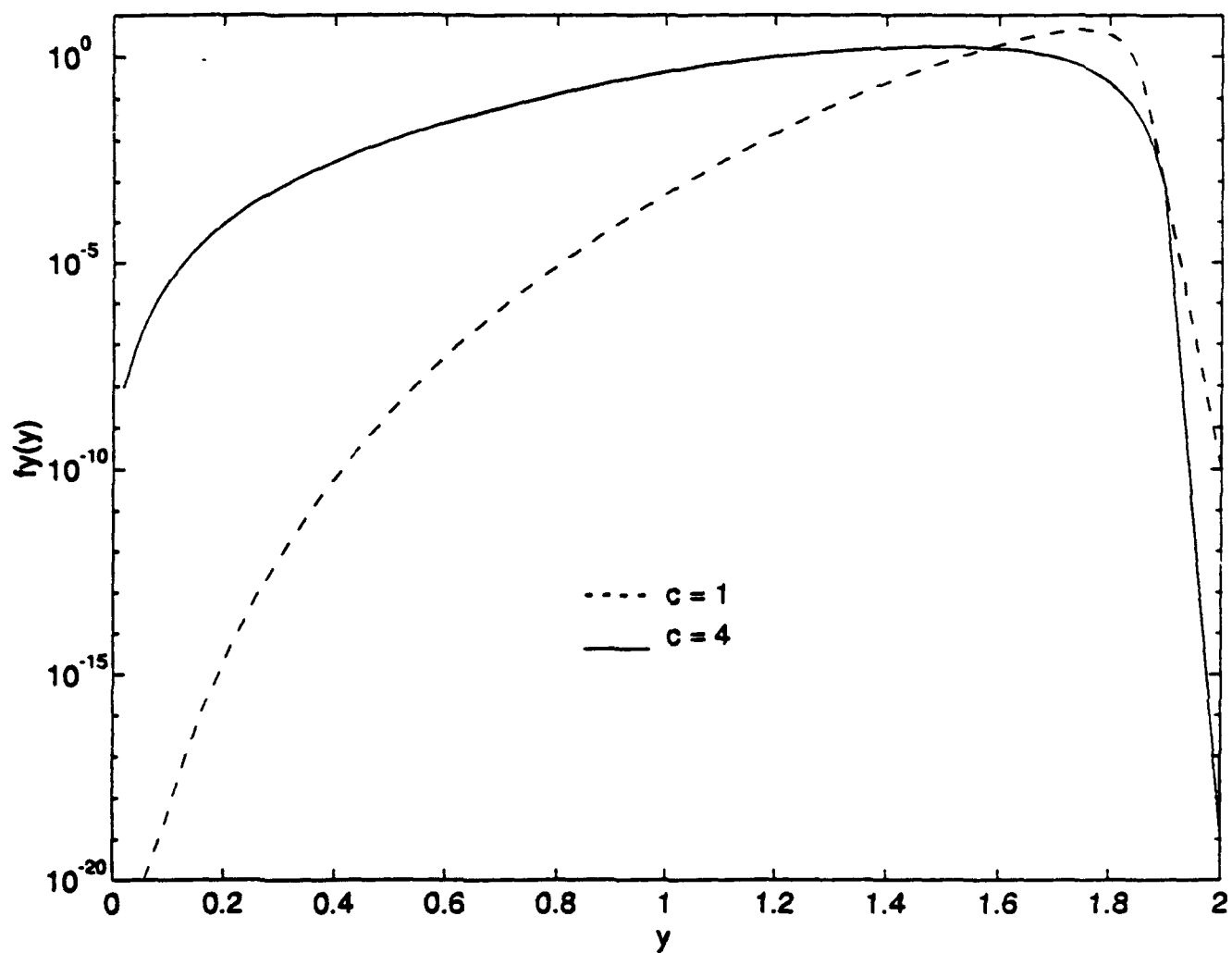
Figure 7: Probability density function of y for $M = 2$, $c = 1$, and $c = 4$.
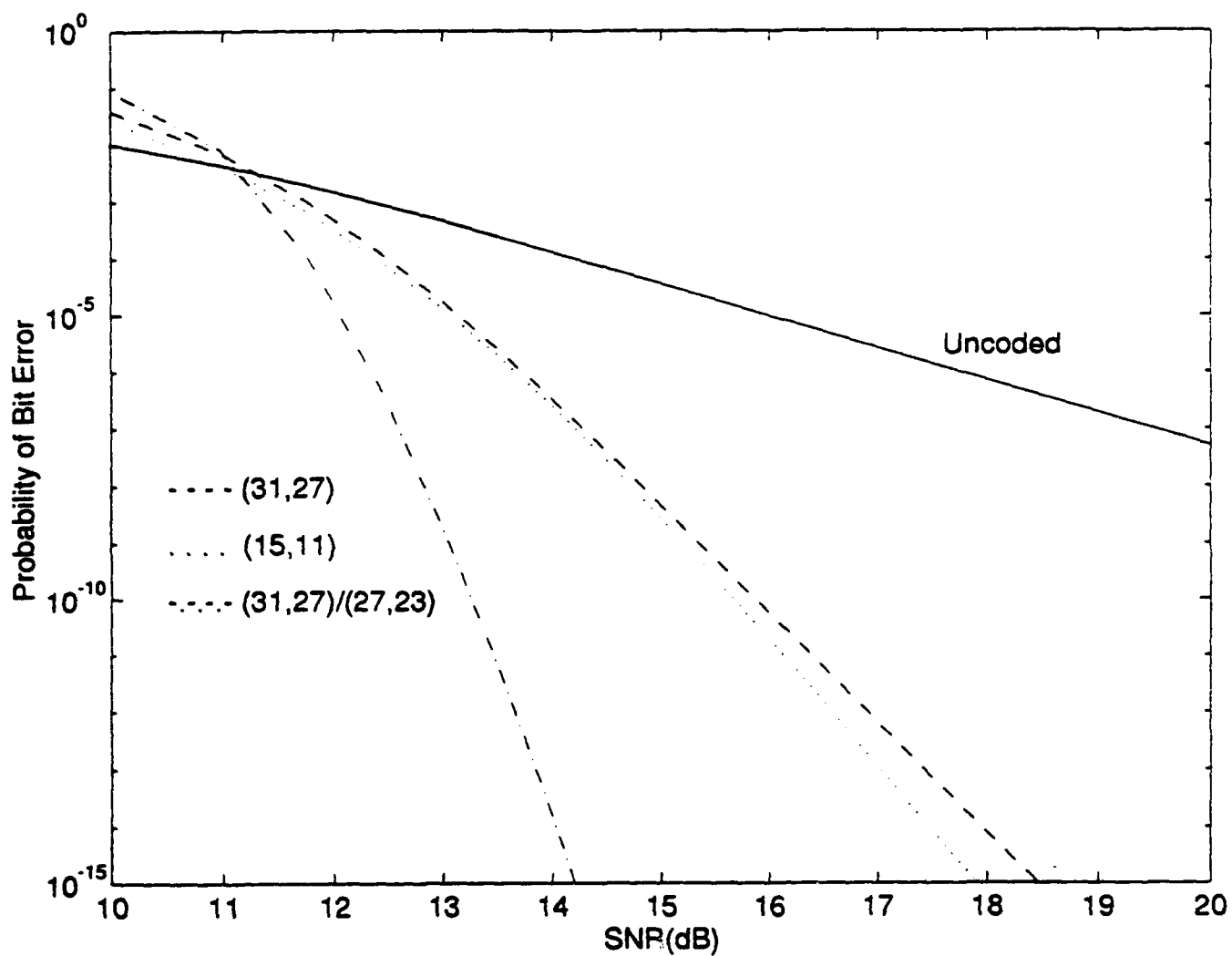
Figure 8: Coded P_b versus SNR for coherent optical systems employing the (15, 11) and (31, 27) Reed-Solomon codes and the concatenated (31, 27)/(27, 23) Reed-Solomon/Reed-Solomon codes with $M = 1$ and $c = 1$.

20
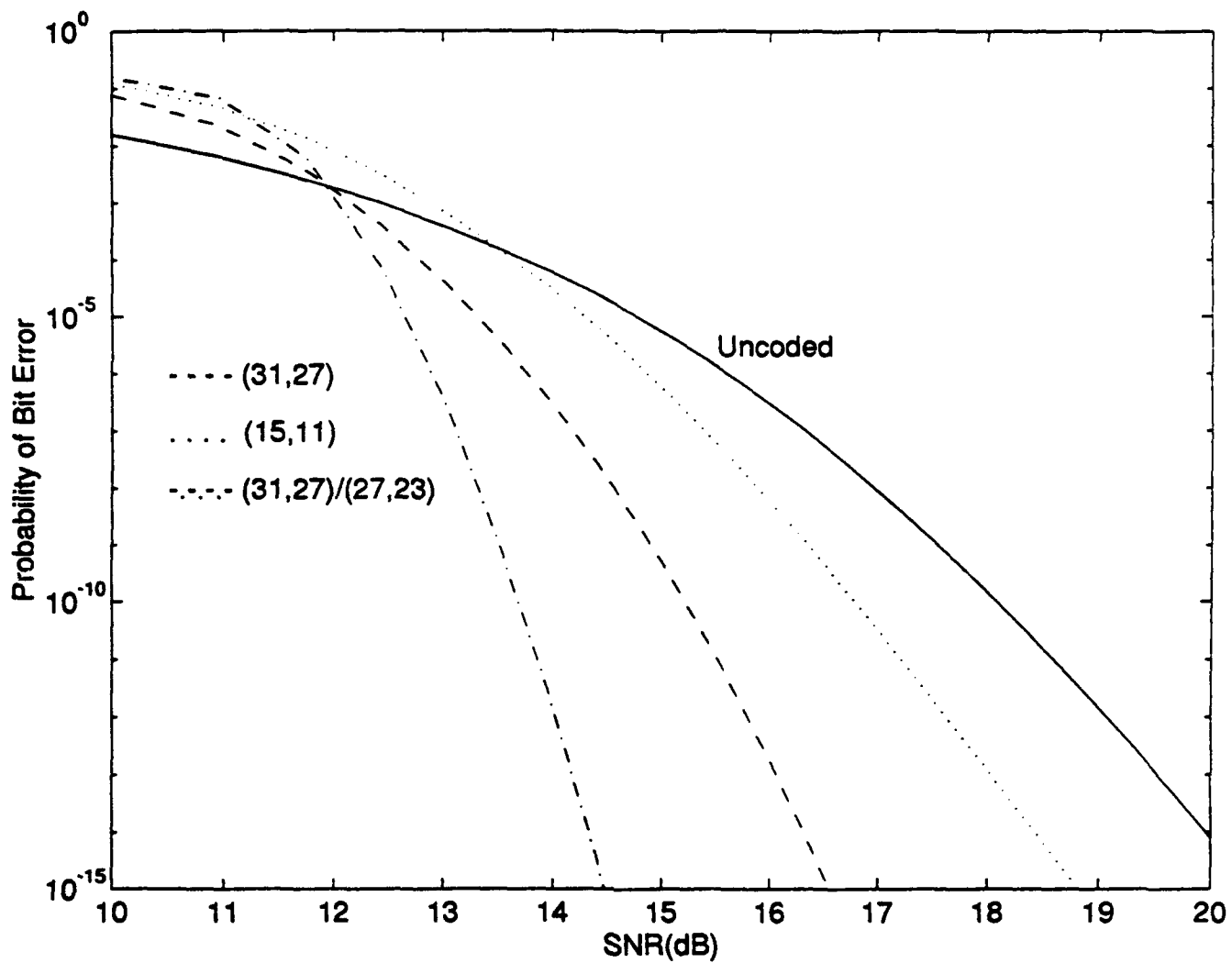
Figure 9: Coded P_b versus SNR for coherent optical systems employing the (15, 11) and (31, 27) Reed-Solomon codes and the concatenated (31, 27)/(27, 23) Reed-Solomon/Reed-Solomon codes with $M = 2$ and $c = 1$.

21
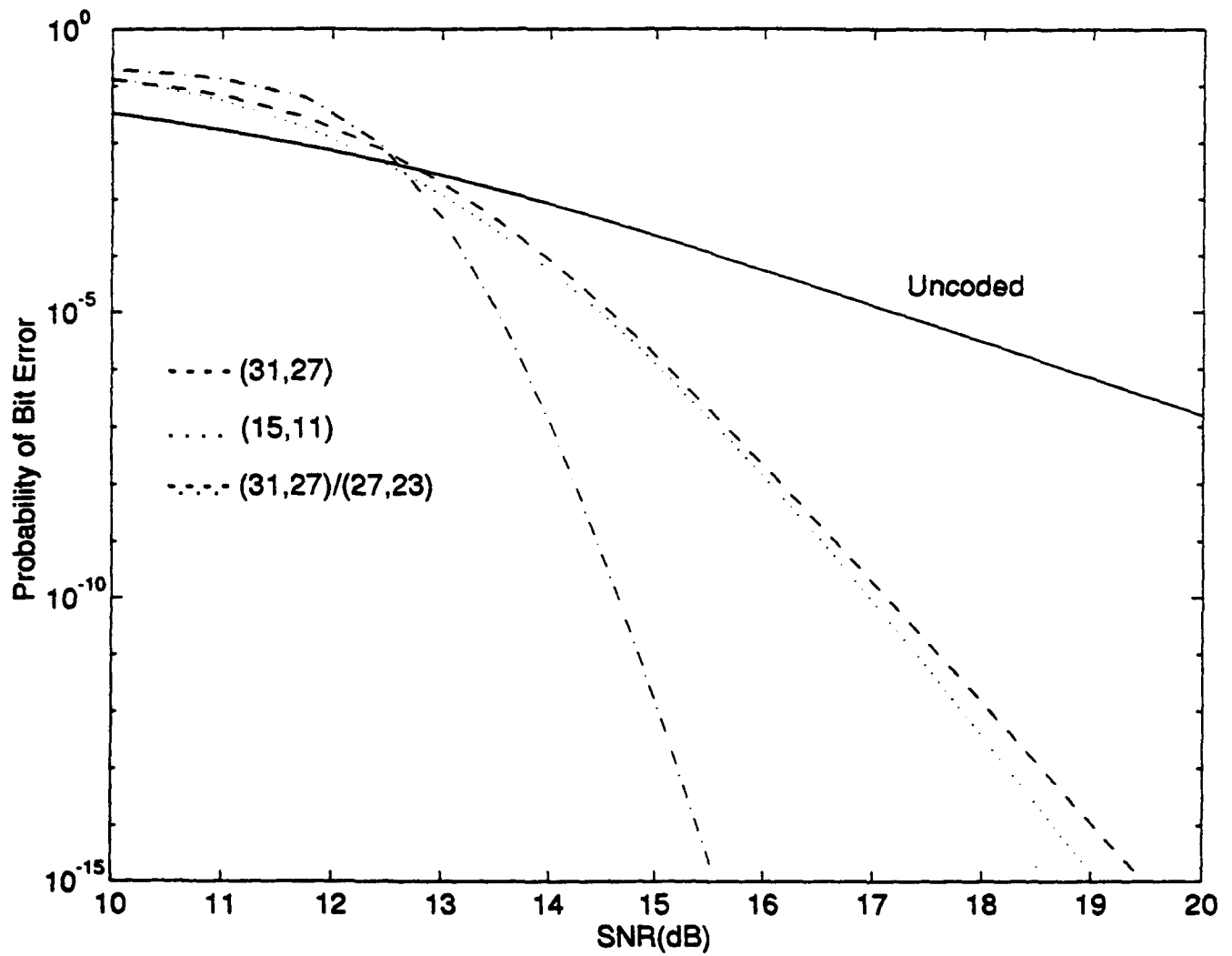
Figure 10: Coded P_b versus SNR for coherent optical systems employing the (15, 11) and (31, 27) Reed-Solomon codes and the concatenated (31, 27)/(27, 23) Reed-Solomon/Reed-Solomon codes with $M = 2$ and $c = 4$.

22
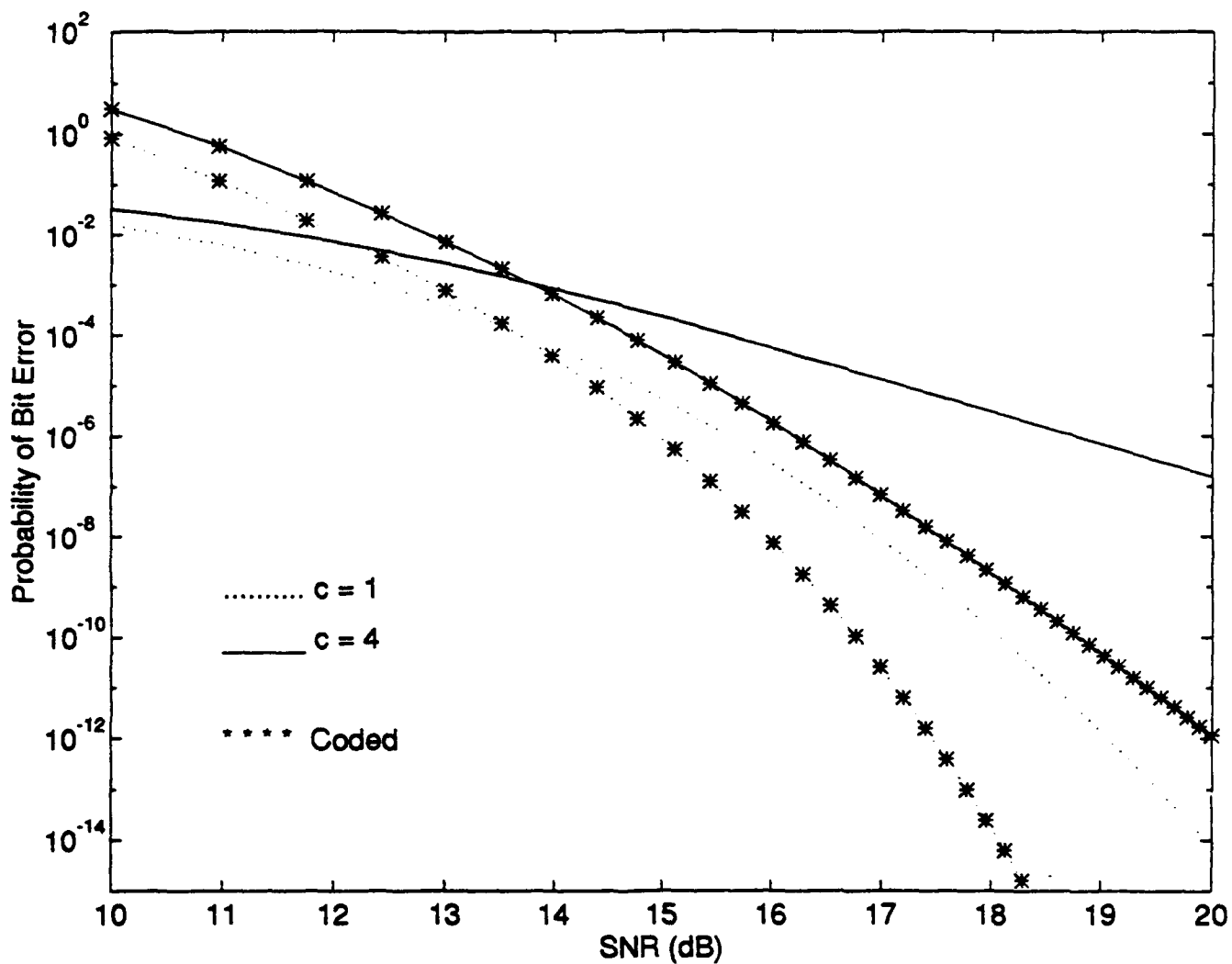
Figure 11: Coded P_b versus SNR for coherent optical systems employing hard decoding convolutional code with rate 3/4 and constraint length 2, $M = 2$, $c = 1$ and $c = 4$.
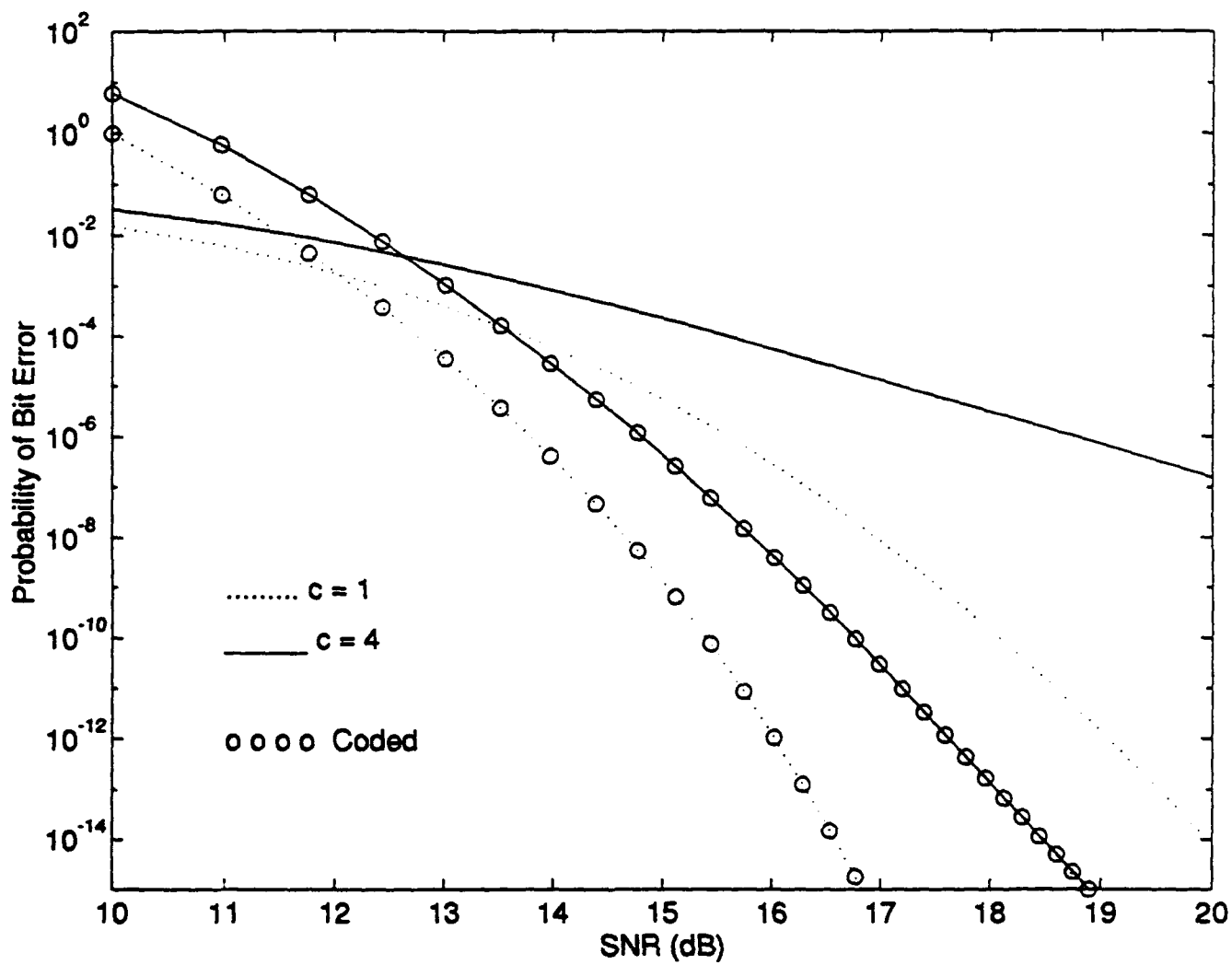
Figure 12: Code P_b versus SNR for coherent optical systems employing hard decoding convolutional codes with rate 3/4 and constraint 5, $M = 2$, $c = 1$ and $c = 4$.

24

IV. CONCLUSIONS

From our investigaion we conclude that error correction coding can improve the performance of both direct detection and coherent optical systems. The improvement is considerable when concatenated codes are used. From the practical point of view, short RS codes with modest error correcting capability can be concatenated to provide large coding gain and at the same time can be implemented at high data rates. Convolutional codes with soft decision also provides good coding gain at moderate data rates for direct detection systems. It remains to be seen how much coding gain can be obtained with soft decision convolutional codes for coherent optical systems.

Our contributions in this thesis are the numerical results obtained from the analytical work in [19] as shown in equations (1–31).

APPENDIX

The following MATHEMATICA (Stephen Wolfram, 1993) and MATLAB (The Math Works, 1993) codes offer the formulations for:

The convol: ion method for the determination of the probability density function

The computation of bit error probability for direct detection and coherent detection

1. *Obtaining of pdf of y by M-fold convolution*

```
x1=[.......]          ......................Convolution method for finding pdf of y
                      .................Input of pdf of x
x2=x1;        ...........................x1,x2 are i.i.d
x3=0:0.02:2;
y1=0.02*conv(x1,x2);    .............0.02 is integer as interval
                 ...................2nd convolution
```

2. Bit error probability for direct detection

2.1 Uncoding case

```
function y=q(x)         .........Definition of q(x) in MATLAB
y=0.5*erfc(x/sqrt(2))   ...........Use error function defaulted in
                                  MATLAB
snrdb=6.5:0.02:12.1;
snr=10.^(snrdb*0.1);
pu=q(snr*0.5);          ..........Uncode case
```

2.2 Concatenated convolutional hard and soft/RS coding

```
M1=input('input inner convolution code order as n,k,v,df,wd,wd+1...');
                 ................Need to input
                                two matrix,one for RS code(outter),
                                one for convolution (inner)
M2=input('input outter RS code as n,k');
n1=M1(1); k1=M1(2); n2=M2(1);   k2=M2(2);
r1=k1/n1; r2=k2/n2;
m2=log2(n2+1); t2=(n2-k2)*0.5;
```

```
r=r1*r2;
p=q(snr*r^0.5*0.5);          ...............Equation (7)
     pj1=[];    ......................Solve five pj values
                                      Hard   case
     pj2=[];        ..............   Soft   case
     for d=0:4
      pj=0;
      j=M1(4)+d;
      if rem(j,2)==1   ...............Check odd or even case
         for i=(j+1)/2:j
              pj=pj+bino(j,i)*p.^i.*(1-p).^(j-i);
                 end
      else
          for i=j/2+1:j
          pj=pj+bino(j,i)*p.^i.*(1-p).^(j-i);
                  end
          pj=pj+0.5*bino(j,0.5*j)*p.^(0.5*j).*(1-p).^(0.5*j);
      end
      pj1=[pj1;pj];     ......................  Hard   case's  pj
         ppjj=q(  (r*j)^0.5*snr*0.5);  .........Soft case's pj
         pj2=[pj2;ppjj];
     end
      pb_conv=0;   .................Solve for pb for hard case
      ppbb_conv=0;   .................For soft case
      for h=1:5   ...................5 is from wd to wd+4
       pb_conv=pb_conv+M1(h+4)*pj1(h,:);
          ppbb_conv=ppbb_conv+M1(h+4)*pj2(h,:);
      end
      pb_conv=pb_conv/k1;
      ppbb_conv=ppbb_conv/k1;
      ps=1-(1-pb_conv).^m2;   ........Solve for ps
      ppss=1-(1-ppbb_conv).^m2;
      pb=0; ppbb=0;   .................Solve for pb
      for j=t2+1:n2
     pb=pb+(j+t2)/n2*bino(n2,j)*ps.^j.*(1-ps).^(n2-j);
     ppbb=ppbb+(j+t2)/n2*bino(n2,j)*ppss.^j.*(1-ppss).^(n2-j);
         end
      pb=pb*(n2+1)/(2*n2);
      ppbb=ppbb*(n2+1)/(2*n2);
      ss=linspace(1,len,51);   .........Plot statement
      semilogy (snrdb(ss), pu(ss),'*',snrdb,pb,'--',snrdb,ppbb)
      axis([snrdb(1) snrdb(len) 10^(-15) 1])
```

3. Bit error probability for coherent detection

3.1 Uncoding case

```
y11={.................}     ..........Input pdf value of y
M=2;
S=55;        ...........................Wanted  SNR
```

```
y1=Table[y,{y,0.01761,1.9,0.02}];
p1=Table[Sum[(((S*y)/(2*M))^n)/(n!)
*Sum[Binomial[M+k-1,k-n]
*(2^(-k)),{k,n,M-1}],{n,0,M-1}]
*Exp[-(S*y/(2*M))]/(2^M),
{y,0.01761,1.9,0.02}];
p2=Table[{y1[[i]],p1[[i]]*y11[[i]]},
{i,1,Length[y1]}];
p3=Interpolation[p2, InterpolationOrder -> 1]
                    ..................  Connect each point
p4=NIntegrate[p3[y],{y,0.01761,1.89761}]
```

3.2   concatenated RS/RS coding

```
y11={...........};     ................For coding case's pdf of y value
For[M=1; g=1;  n1=31; n2=27; k1=27; k2=23; rc1=k1/n1;
rc2=k2/n2; S1=10;      ................Inputs of SNR  and code rate
S=S1*rc1*rc2, S +=5,
y1=Table[y,{y,0.04283,0.97772,0.02}];
p1=Table[Sum[(((S*y)/(2*M))^n)/(n!)
*Sum[Binomial[M+k-1,k-n]
*(2^(-k)),{k,n,M-1}],{n,0,M-1}]
*Exp[-(S*y/(2*M))]/(2^M),
{y,0.04283,0.97772,0.02}];
p2=Table[{y1[[i]],p1[[i]]*y11[[i]]},
{i,1,Length[y1]}];
p3=Interpolation[p2, InterpolationOrder -> 1];
p4=NIntegrate[p3[y],{y,0.04283,0.96283}];
Print[p4]]
```

3.3   Convolutional coding

```
p=[..............];     ................Input p
len=length(p);
M=[4,3,2,3,15,104,540,2520,11048];  .........Matrix order as
                                    n,k,v,df,wd,wd+1,wd+2,...

r=M(2)/M(1);   ........................Solve for convolution code in
                                    matrix
pj1=[..............];      ...........Solve five Pj values
for d=0:4   ..........................d   i.e., df which value depend on
                                    weight wd+4
pj=0;
pj=M(4)+d;
 if  rem(j,2)==1   ................Check odd or even case
 for i=(j+1)/2:j
 pj=pj+bino(j,i)*p.^i.*(1-p).^(j-i);
 end
```

29

```
  else
for i=j/2+1:j
pj=pj+bino(j,i)*p.^i.*(1-p).^(j-i);
end
pj=pj+0.5*bino(j,0.5*j)*p.^(0.5*j).*(1-p).^(0.5*j);
end
pj1=[pj1;pj];
end
pb=0;
for h=1:5
pb=pb+M(h+4)*pj1(h,:);
end
pb=pb/M(2);
plot(s,pb)              ..................Plot statement
```

REFERENCES

[1] Viberbi, A. J., and Omura, J. K., *Principles of Digital Communication and Coding*, New York: McGraw-Hill, 1979.

[2] Lin, S., and Costello, D. J., *Error Control Codeing: Fundamentals and Applications*, Englewood Cliffs, NJ: Prentice-Hall, 1983.

[3] Clark, G. C., and Cain, J. B., *Error-Correction Coding for Digital Communications*, New York: Plenum Press, 1988.

[4] Wu, J., "Coding to Relax Laser Linewidth Requirements and Improve Receiver Sensitivity for Coherent Optical BPSK Communications," *J. Lightwave Technol.*, Vol. 8, No. 4, pp. 545–553, Apr. 1990.

[5] Grover, W. D., "Forward Error Correction in Dispersion-Limited Lightwave Systems," *J. Lightwave Technol.*, Vol. 6, No. 5, pp. 643–654, May 1988.

[6] Saltz, J., "Coherent Lightwave Communications," *AT&T Tech. J.*, Vol. 64, pp. 2153–2209, Dec. 1985.

[7] Kazovsky, L. G., "Impact of Phase Noise on Optical Heterodyne Communication Systems," *J. Opt. Commun.*, Vol. 7, No. 2, pp. 66–78, 1986.

[8] Kikuchi, K., "Degradation of Bit Error Rate in Coherent Optical Communications Due to Spectral Spread of the Transmitter and the Local Oscillator," *J. Lightwave Technol.*, Vol. LT-2, pp. 1024–1033, Dec. 1984.

[9] Garrett, I., and Jacobsen, G., "Theoretical Analysis of Heterodyne Optical Receivers for Transmission Systems Using (Semiconductor) Lasers with Non-negligible Linewidth," *J. Lightwave Technol.*, Vol. LT-4, pp. 323–324, Mar. 1986.

[10] Barry, J. R., and Lee, E. A., "Performance of Coherent Optical Receivers," *Proc. IEEE*, Vol. 78, No. 8, pp. 1369–1394, Aug. 1990.

[11] Foschini, G. J., "Noncoherent Detection of Coherent Lightwave Signals Corrupted by Phase Noise," *IEEE Trans. Commun.*, Vol. 36, pp. 306–314, Mar. 1988.

[12] Azizoglu, M., and Humblet, P. A., "Envelope Detection of Orthogonal Signals with Phase Noise," *J. Lightwave Technol.*, Vol. 9, No. 10, pp. 1398–1410, Oct. 1991.

[13] Kazovsky, L. G., "ASK Multiport Optical Homodyne Receivers," *J. Lightwave Technol.*, Vol. LT-5, pp. 770–791, Jun. 1987.

[14] Proakis, J. G., *Digital Communications*, 2nd ed., New York: McGraw-Hill, 1989.

[15] Gradshteyn, I. S., and Ryzhik, I. M., *Tables of Integrals, Series, and Products, Corrected and Enlarged Edition*, New York: Academic Press, 1980.

[16] Kazovsky, L. G., and Tonguz, O. K., "ASK and FSK Coherent Lightwave Systems: A Simplified Approximate Analysis," *J. Lightwave Technol.*, Vol. 8, No. 3, pp. 338–352, Mar. 1990.

[17] Forchini, G. J., "Envelope Statistics for Filtered Optical Signals Corrupted by Phase Noise," *IEEE Trans. Commun.*, Vol. 37, No. 12, pp. 1293–1302, Dec. 1989.

[18] Okoshi, T., and Kikuchi, K., *Coherent Optical Fiber Communications*, Tokyo, Japan: KTW Scientific (and Kluwer Academic), 1988.

[19] Ha, T. T., "Coded Lightwave Systems," research notes, Sep. 1993.

INITIAL DISTRIBUTION LIST

		No. Copies
1.	Defense Information Center Cameron Station Alexandria, VA 22304-6145	2
2.	Library Code 52 Naval Postgraduate School Monterey, CA 93943-5002	2
3.	Acting Chairman, Code PH/Sd Engineering Acoustic Academic Committee Naval Postgraduate School Monterey, CA 93943-5000	1
4.	Professor Tri T. Ha, Code EC/Ha Department of Electrical and Computer Engineering Naval Postgraduate School Monterey, CA 93943-5121	2
5.	Professor Randy L. Borchardt, Code EC/Bt Department of Electrical and Computer Engineering Naval Postgraduate School Monterey, CA 93943-5000	2
6.	Hwang, Eui-Sik LT, R.O.K. Navy Woo-Nam-Dong 492-39, Buk-Gu Kwang-Ju City, Republic of Korea	5